Journal of proteome research

Article

pubs.acs.org/jpr

Systematic Protein Level Regulation via Degradation Machinery Induced by Genotoxic Drugs

Kohei Kume,[†,‡,§,∥] Kazushige Ishida,[†,‡] Miyuki Ikeda,[†,‡] Kazuhiro Takemoto,[#] Tsutomu Shimura,[▽] Lynn Young,[○] and Satoshi S. Nishizuka*[,†,‡,§,∥,⊥]

[†]Molecular Therapeutics Laboratory, [‡]Department of Surgery, Iwate Medical University School of Medicine, Morioka, Iwate 020-8505, Japan

[§]Medical Innovation for Advanced Science and Technology program (MIAST), Iwate Medical University, Morioka, Iwate 020-8505, Japan

[∥]Institute for Biomedical Sciences, Iwate Medical University, Yahaba, Iwate 020-8505, Japan

[⊥]Department of Surgery, Iwate Medical University School of Dentistry, Morioka, Iwate 020-8505, Japan

[#]Department of Bioscience and Bioinformatics, Kyushu Institute of Technology, Iizuka, Fukuoka 820-8502, Japan

[▽]Department of Environmental Health, National Institute of Public Health, Wako-shi, Saitama 351-097, Japan

[○]National Institutes of Health (NIH) Library, Division of Library Services, Office of Research Services, National Institutes of Health, Bethesda, Maryland 20892, United States

Supporting Information

ABSTRACT: In this study we monitored protein dynamics in response to cisplatin, 5-fluorouracil, and irinotecan with different concentrations and administration modes using "reverse-phase" protein arrays (RPPAs) in order to gain comprehensive insight into the protein dynamics induced by genotoxic drugs. Among 666 protein time-courses, 38% exhibited an increasing trend, 32% exhibited a steady decrease, and 30% fluctuated within 24 h after drug exposure. We analyzed almost 12,000 time-course pairs of protein levels based on the geometrical similarity by correlation distance (*dCor*). Twenty-two percent of the pairs showed *dCor* > 0.8, which indicates that each protein of the pair had similar dynamics. These trends were disrupted by a proteasome inhibitor, MG132, suggesting that the protein degradation system was activated in response to the drugs. Among the pairs with high *dCor*, the average *dCor* of pairs with apoptosis-related protein was significantly higher than those without, indicating that regulation of protein levels was induced by the drugs. These results suggest that the levels of numerous functionally distinct proteins may be regulated by common degradation machinery induced by genotoxic drugs.

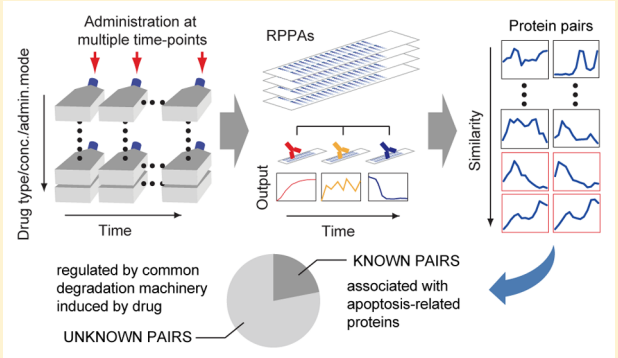

KEYWORDS: *protein dynamics, cancer cell, genotoxic drug, reverse-phase protein microarray (RPPA), correlation distance (dCor)*

INTRODUCTION

Anticancer drugs induce either cytotoxic or cytostatic effects to suppress tumor growth. These effects are thought to result from the activation of either cell death or cell cycle arrest pathways. Although the mechanism of action of cancer drugs can be thought of in such simple terms, in reality their antitumor effects are often much more complex, particularly when analyzed at the protein level.[1,2] In fact, the activation of pro-apoptotic and cell cycle arrest pathways are altered depending on the type, concentration, and method of administration of anticancer drugs as well as the underlying genomic aberrations present and the intrinsic gene expression pattern of the cell lineage. However, little is known about the collective changes that are manifested by dynamics in protein levels as a result of drug administration, since this requires labor-intensive sample collection, large-scale experiments, and the development of algorithms for high-dimensional data mining.[3]

To address whether the protein dynamics in response to various drug treatments are indicative of reactions unique to drug input, we employed a "reverse-phase" protein lysate microarray (RPPA), which is a microscale "dot" blot that can monitor protein levels across more than 10,000 data points under a single experimental condition (Figure 1A).[4−6] In the current study, we used three genotoxic stress agents (5-fluorouracil, 5FU; cisplatin, CIS; and irinotecan, CPT) frequently used for cancer treatment at three concentrations (high, medium, and low) and applied two different administration modes (sustained and temporal) over a

Received: August 17, 2015
Published: December 1, 2015

DOI: 10.1021/acs.jproteome.5b00759
J. Proteome Res. 2016, 15, 205−215

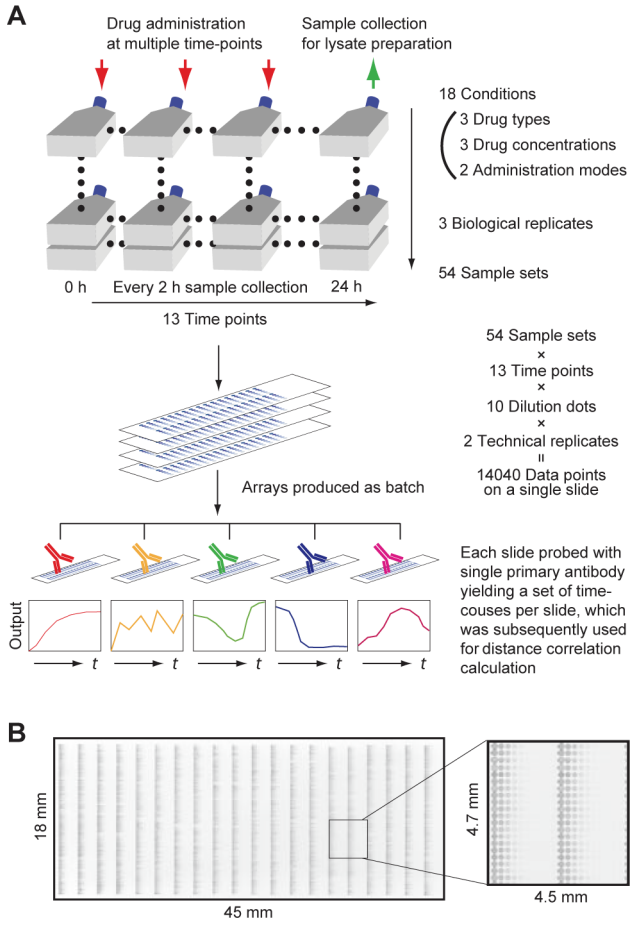

Figure 1. High-dimensional protein monitoring system using RPPAs. (A) A flow diagram of the time-course experiment. Cells were cultured up to 80% confluency in flasks for the required time points. Drugs were added at designated time points, and the cells were collected at the end of each experiment so that cell proliferation effects were minimized. Cell lysate from each flask was prepared according to previously published protocols. All cell lysates were printed on nitrocellulose membranes by an automated protein microarrayer (Aushon 2470). The produced RPPAs were probed with previously screened primary antibodies followed by quantitative immunochemical detection. A digital imaging process generated quantitative protein expression over 18 different conditions. t = time. (B) Actual image of an RPPA. The inset indicates a section printed by a single pin showing a set of lysates from different time points printed in 2-fold serial dilutions with a duplicate print (each row represents the dilution series of a lysate from a single sample-collection point).

24-h time-course on the HCT116 colon cancer cell line (Figure 1B and Table 1). Specific antibodies on an RPPA were used to monitor the dynamics of 37 proteins chosen based on their involvement in diverse functional pathways, including cell structure, cell growth, stress response, apoptosis, and cell cycle. Importantly, antibodies against these proteins were screened to produce single predominant bands at expected molecular weights by Western blot for quantitative image analysis on RPPA (Figure S1 and Table S1, Supporting Information).[4,7,8] More than 1,800 protein dynamics were subsequently analyzed based on pairwise correlation distance ($dCor$),[9,10] by which geometrical similarities of two given dynamics were calculated. Geometrical similarities do not always directly indicate that a pair of proteins interacts; however, highly coexpressed proteins that form a functional module in response to drugs may be associated with the intrinsic molecular entity of the cells.[11−15] Thus, based on the concept of cell-drug profiling, we attempted to answer the following research questions: (i) What type of trends in protein dynamics are induced by each drug?; and (ii) What mechanisms regulate the protein dynamics over time after genotoxic drug administration?

Table 1. Summary of Experimental Conditions

Parameters	No. data points; description
Cell type	1; HCT116
Drug	3; 5FU, CIS, CPT
Concentration	3; high, medium, low
Administration method	2; sustained and temporal
Time points	13; 0−24 h, every 2 h
Experimental replicates	3; triplicate culture flasks
Technical replicates	2; duplicate prints

MATERIALS AND METHODS

Sample Collection

The colon cancer cell line HCT116 was selected for use in the present study based on the following reasons: (i) It is one of the well-characterized cell lines in the literature; (ii) the growth is relatively fast; and (iii) the DNA damage response has been well studied using RPPA. Hence, the HCT116 cell line is suitable for a large-scale sample collection; and the specificity of a large number of antibody sets is guaranteed to work for RPPA analysis.[4,7,8] The technical difficulties are minimized related to the sample number, RPPA fabrication and analysis. For the sample collection, the cell line HCT116 cells was exposed to genotoxic anticancer drugs (5FU, CIS, CPT) in T-25 flasks at low (L), medium (M), and high (H) concentrations. The medium (M) concentration of each drug was defined as the concentration that caused 50% growth suppression (GI_{50}) relative to the no-drug condition for each drug. The high (H) concentrations were 10-fold (for 5FU and CIS) or 100-fold (for CPT) higher than M. Each concentration was applied in both temporal (tem) and sustained (sus) modes for 13 time points over 24 h. For the sustained mode of drug administration, the drug was kept in the medium until the end of the experiment (24 h), whereas it was removed after 4 h for the temporary mode. These conditions were determined by an extensive optimization study using conventional Western blot prior to RPPA experiment (Figure S2, Supporting Information). The experimental design is summarized in Figure 1A. Thus, there were 18 different conditions in total. The low (L) concentrations were 10-fold (for 5FU and CIS) or 100-fold (for CPT) lower than M. Cells were collected by manual scraping and centrifuged at 1,700 g for 2 min at 4 °C. The resulting cell pellet was stored at −80 °C for further RPPA analysis as previously described.[4,6]

RPPA

Cell pellets were processed to obtain cell lysates according to previously published protocols.[6] An individual RPPA contains 14,040 dots of 18 conditions ×13 time-courses, and 1,160 dots of control MIX samples[4,7,8] produced with the Aushon 2470 Microarrayer (Aushon BioSystems, MA) on nitrocellulose-embedded glass slides (Grace BioLabs, OR). The Mix sample was made of a variety of sample lysates from all possible drug administrative conditions. Thus, the MIX sample provides a good representation of the differences of protein levels in the drug administrative conditions used in this study. Each sample lysate was spotted in 2-fold serial dilutions in 10 replicates for

DOI: 10.1021/acs.jproteome.5b00759
J. Proteome Res. 2016, 15, 205−215

quantitative analysis (Figure 1B) and subsequently probed with individual primary antibodies, whose specificity had been verified by strip Western blotting.[4,7,8] For blocking unspecific interactions, SuperG (Grace Biolabs), iBlock (Life Technologies, NY), or standard BSA solutions were used depending on the antibody. The signal was obtained using immunohistochemical agents such as Tyramide Signal Amplification (Dako Cytomaitons, CA), which subsequently was quantified using a P-scan program followed by the DI_{25} algorithm for a final value output.[4,16]

Quality Control of RPPA

Reproducibility was measured by control samples (MIX, 0-time point) against all antibodies used. The average coefficient of variation (CV) was 16.6% for MIX and 19.8% for the 0-time point, which is consistent with previous studies.[4,17]

Specificity of Primary Antibodies

All primary antibodies were tested for specificity using strip Western blot as per previously published criteria.[7,8] The list of antibodies and the results of the strip Western blots are shown in Table S1 and Figure S1, respectively (Supporting Information).

RPPA Data Processing

Principal component analysis (PCA) was used to remove systematic bias effects of immunostaining. The systematic bias effects generate more variation than any single factor, as measured by the sum of squares.[18] We hypothesized that there may be some common components in protein expression due to nonspecific (irrelevant to primary antibody) staining effects across RPPA slides stained with different primary antibodies.

Based on this hypothesis, the PCA model can be expressed as

$$X = AB$$

where X is an $M \times N$ matrix consisting of the raw DI_{25} data subjected to PCA analysis.[4] M is the number of protein species, while N is the number of time points with experimental replicates. A is an $M \times K$ matrix that contains protein species in its rows and different conditions in its columns. B is a $K \times N$ matrix, whose rows represent the conditions and columns of protein levels derived from triplicate data per time point.

The goal of the PCA was to detect "variation trends" across different proteins. To do so, calculations for PCA were repeated until the PCA distribution fell within 2.5 standard deviations by repeatedly removing outliers. After determining PCA in the final subset that was considered to be the bias component, it was used to adjust each data set. The final time-course data set was generated from the PCA-adjusted data (Figure S3, Supporting Information). Since the PCA-adjusted data set was still assumed to include stochastic noise independent of experimental bias, which can be seen as a variation between experimental replicates, we subsequently applied a random walk Markov Chain Monte Carlo (MC/MC) algorithm to smooth protein expression as a function of time with time point by time point fluctuations.[19] All calculations were executed using the R statistical package.

Classification of Protein Dynamics Profiles

A total of 666 time-course data points were classified by K-means clustering using Genesis software (http://genome.tugraz.at).[20] Reproducibility of results was confirmed by repetitive independent calculations. The number of classifications was empirically determined using the average silhouette score[11] and average-linkage hierarchical clustering[21,22] using Matlab (MathWorks, MA) and CIMminer (http://discover.nci.nih.gov/cimminer/) software, respectively.

Distance Correlation

Conventional Pearson correlation coefficient measures linear dependence between two random variables; thus it may not always be sufficient for measuring nonlinear or nonmonotone dependence, such as time series. Distance correlation ($dCor$) is a dependence coefficient that measures various kinds of dependence between two random vectors in arbitrary dimension. It has been shown that $dCor$ is superior for nonlinear relationships over the conventional Pearson correlation coefficient.[9,10] For the present data, $dCor$ indicates distance between two metrices (two time-course data points) comprised of protein level p and discrete time points t. The distance covariance ($dCov$) between random variables X and Y for the time-course data set is the square root of

$$dCov_n^2(X, Y) = \frac{1}{n^2} \sum_{p,t=1}^{n} X_{pt} Y_{pt}$$

where X_{pt} and Y_{pt} are pairwise protein amounts as a 2-dimensional function of time. Similarly, distance variance ($dVar$) is defined as the square root of

$$dVar_n^2(X) = dCov_n^2(X, X) = \frac{1}{n^2} \sum_{p,t=1}^{n} X_{p,t}^2$$

Hence, the empirical $dCor$ (X, Y) is given by using sample $dCov$ (X, Y),

$$dCor_n^2(X, Y) = \frac{dCov_n^2(X, Y)}{\sqrt{dCov_n^2(X, X) dCov_n^2(Y, Y)}}$$

where

$$dCor(X, Y) = \frac{dCov(X, Y)}{\sqrt{dCov(X, X) dCov(Y, Y)}}$$

Thus, $dCor$ represents the similarity between two-dimensional functions.

Graphical Representation of Functional Links between Proteins

Node-edge based circular representation[23] was calculated using the data for a subset of protein pairs that had $dCor$ values >0.80. Matrix P1 and P2 (nodes) were converted to graphics using an optimized Matlab script.

Protein Ontology Enrichment Analysis

The number of edges per node was divided into two groups out of five categories (cell cycle, apoptosis, stress response, cell growth, and cell structure): "protein function of interest" and "others". The Fisher's exact test p-values were calculated based on the fraction of functional categories.

FACS

According to our previously published protocols,[17,24] cells were collected by trypsinization, washed with PBS, and fixed in 70% ethanol at −20 °C. Fixed cells were then centrifuged. The resulting cell pellet was mixed with a staining solution containing 0.05 μg/mL propidium iodide and 0.2 μg/mL RNase A for 15 min at room temperature. DNA content was measured by FACScalibur (BD Biosciences, CA) and analyzed with CellQuest software (BD Biosciences). Cell cycle distribution was also assessed by Tali Cell Cycle Kit (Life Technologies).

DOI: 10.1021/acs.jproteome.5b00759
J. Proteome Res. 2016, 15, 205−215

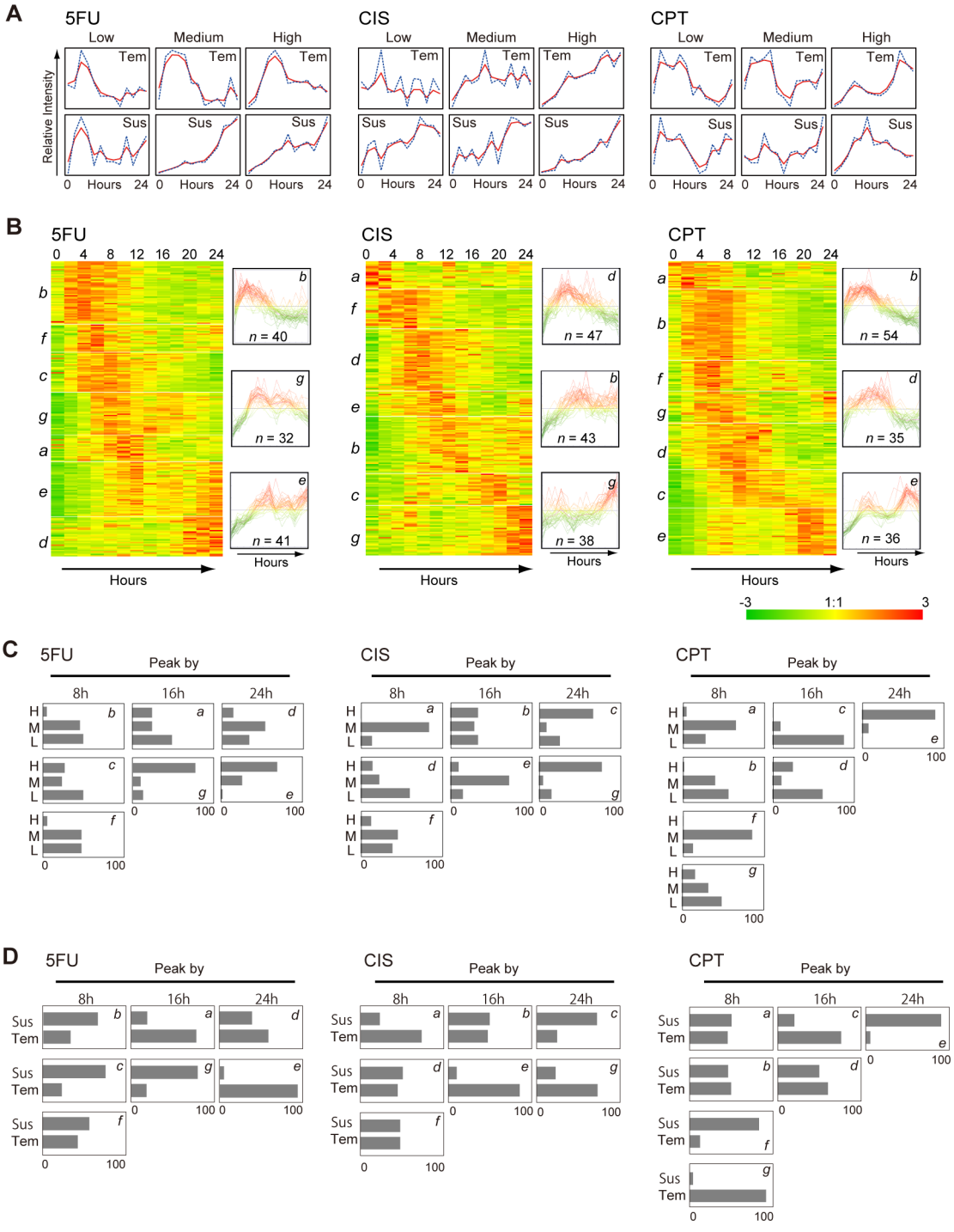

Figure 2. Protein dynamics monitoring. (A) Relative levels of p53 protein were monitored across different conditions. The medium concentration for each drug was set at its GI_{50} (50% growth inhibitory) level, determined using an independent cell-based assay. Sustained administration mode indicates that the drug was never removed from the cell culture medium after addition. Temporal administration indicates that drug was removed after 4 h of exposure. (B) Global protein dynamics profiles after drug exposure. A set of 222 protein dynamics were divided into 7 clusters by the K-means method, which demonstrates a gradual peak shift after drug administration. The set of three panels at the right of each heatmap shows representative geometric patterns of corresponding clusters indicated at the top right. (C) Frequency of protein expression peaks every 8 h for a total of 24 h based on the indicated drug conditions. For instance, after 5FU administration, the majority of cluster *b* proteins show a peak up to 8 h in medium or high drug concentrations. The letter in each box indicates the corresponding cluster in Figure 2B. H, high; M, medium; and L, low drug concentrations. (D) Frequency of protein expression peaks by drug administration modes. For instance, by 5FU administration, the majority of cluster *e* proteins show peaks between 16 and 24 h in temporal administration mode. The letter in each box indicates the corresponding cluster in Figure 2B. Sus, sustained administration mode; and Tem, temporal administration mode.

DOI: 10.1021/acs.jproteome.5b00759
J. Proteome Res. 2016, 15, 205−215

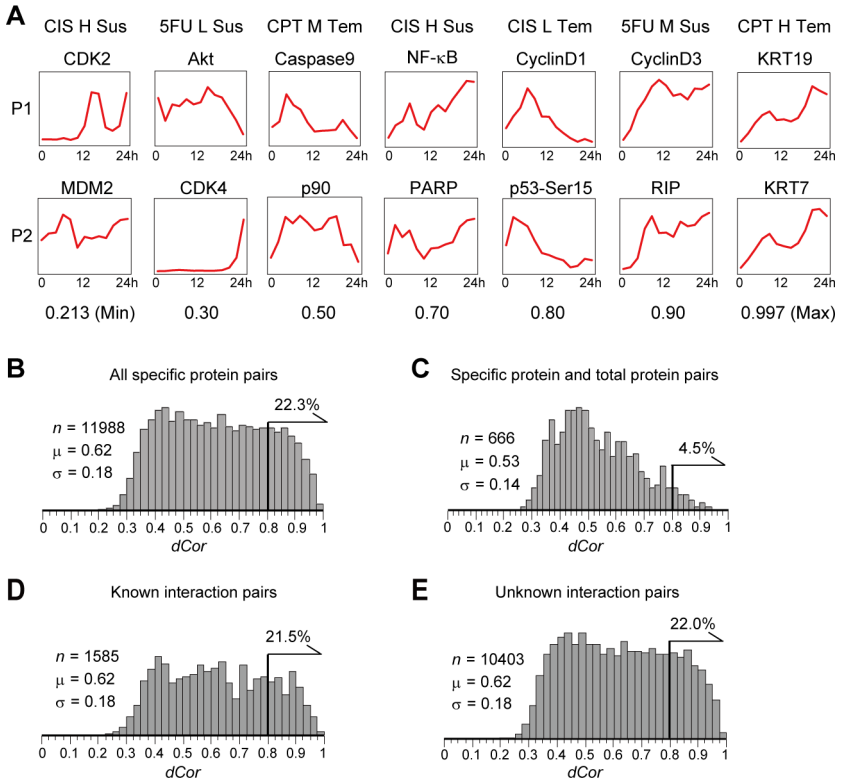

Figure 3. Similarity of protein dynamics. (A) Representative results for protein pairs to be compared geometrically as a function of time. The horizontal axis is time and the vertical axis is relative protein expression. Drug conditions and proteins are indicated at the top of each panel. Distance correlation (*dCor*) values are indicated at the bottom. (B) Distribution of *dCor* values for function-defined protein pairs. The sample numbers (n), the mean (μ), the standard deviation (σ), and the fraction showing a value greater than 0.80 of *dCor* are indicated. (C) Function-defined and total (nonfunctional) protein pairs. The sample numbers (n), the mean (μ), the standard deviation (σ), and the fraction showing a value greater than 0.80 of *dCor* are indicated. (D) Protein pairs whose interaction is known. The sample numbers (n), the mean (μ), the standard deviation (σ), and the fraction showing a value greater than 0.80 of *dCor* are indicated. (E) Protein pairs whose interaction is unknown. The sample numbers (n), the mean (μ), the standard deviation (σ), and the fraction showing a value greater than 0.80 of *dCor* are indicated.

Alteration of Protein Dynamics by Proteasome Inhibitors

Chymotrypsin-like proteasome activity was first investigated in the presence or absence of genotoxic drugs in a 96-well cell-based assay (Promega, WI). To confirm that no excess degrees of genotoxic stress and apoptosis were induced by MG132 (Sigma, MO) itself, the dose-dependent induction of p53, and cleaved PARP and cleaved caspase-3 induction was investigated. Specific primary antibodies for cleaved PARP (#9541), and cleaved caspase-3 (#9661) were purchased from Cell Signaling Technology (Beverly, MA). The 0.1 μM of MG132 was eventually used for continuous exposure of CIS and CPT with the "high" concentrations of 17 μM and 300 μM, respectively, for the following Western blotting. For Western blot analysis, samples were obtained from HCT116 cells after exposure to MG132 and anticancer agents described above at the following time points (0, 6, 12, 18, and 24 h). Lysate preparation, Western blotting, and signal detection were performed as previously described.[17] The resulting blot was incubated with antibodies against p53 (1:800), Akt (1:1000), p21 (1:1000), and CyclinD1 (1:1000). Total protein concentration was adjusted by cell number before cell lysis and confirmed by Ponceau S staining on the Western blot membrane. The dynamics induced by each drug consistent with RPPA data were subject to interpretation if the dynamics were affected by MG132. Band intensities were quantified using ImageJ (http://rsbweb.nih.gov/ij/). Detailed information on antibodies is described in Table S1 (Supporting Information).

RESULTS

Multiplex Protein Dynamics Can Be Monitored in Response to Genotoxic Stress Agents

Prior to the large-scale sample correction,[6] both time- and drug concentration-dependent protein dynamics were investigated using conventional Western blot to determine an appropriate drug administration conditional window (Figure S2, Supporting Information). We also assessed the cell fate with respect to cell cycle distribution in all corresponding drug administration conditions up to 72 h (Figure S4, Supporting Information).

Next, to confirm whether genotoxic stress was properly induced in the cell lysates used in the RPPA system under the selected conditions, the levels of p53, which is one of the hallmarks of a genotoxic stress response, were examined (Figure 2A).[17,25,26] An antimetabolite, 5FU, induced stabilization of p53 with sustained administration at medium and high concentrations, whereas temporal administration only induced a peak at 4 h. These results suggested that the genotoxic stress response was immediately reset following drug removal.

CIS is a DNA cross-linking agent that ultimately induces apoptosis. As expected, p53 levels did not differ between sustained and temporal administration modes when the CIS concentration was high. Low and medium CIS concentrations with sustained administration increased p53 levels with oscillation; however, temporal administration did not induce p53 stabilization. A topoisomerase-I inhibitor, CPT, caused p53 levels to peak within 12 h followed by continuous stabilization

DOI: 10.1021/acs.jproteome.5b00759
J. Proteome Res. 2016, 15, 205−215

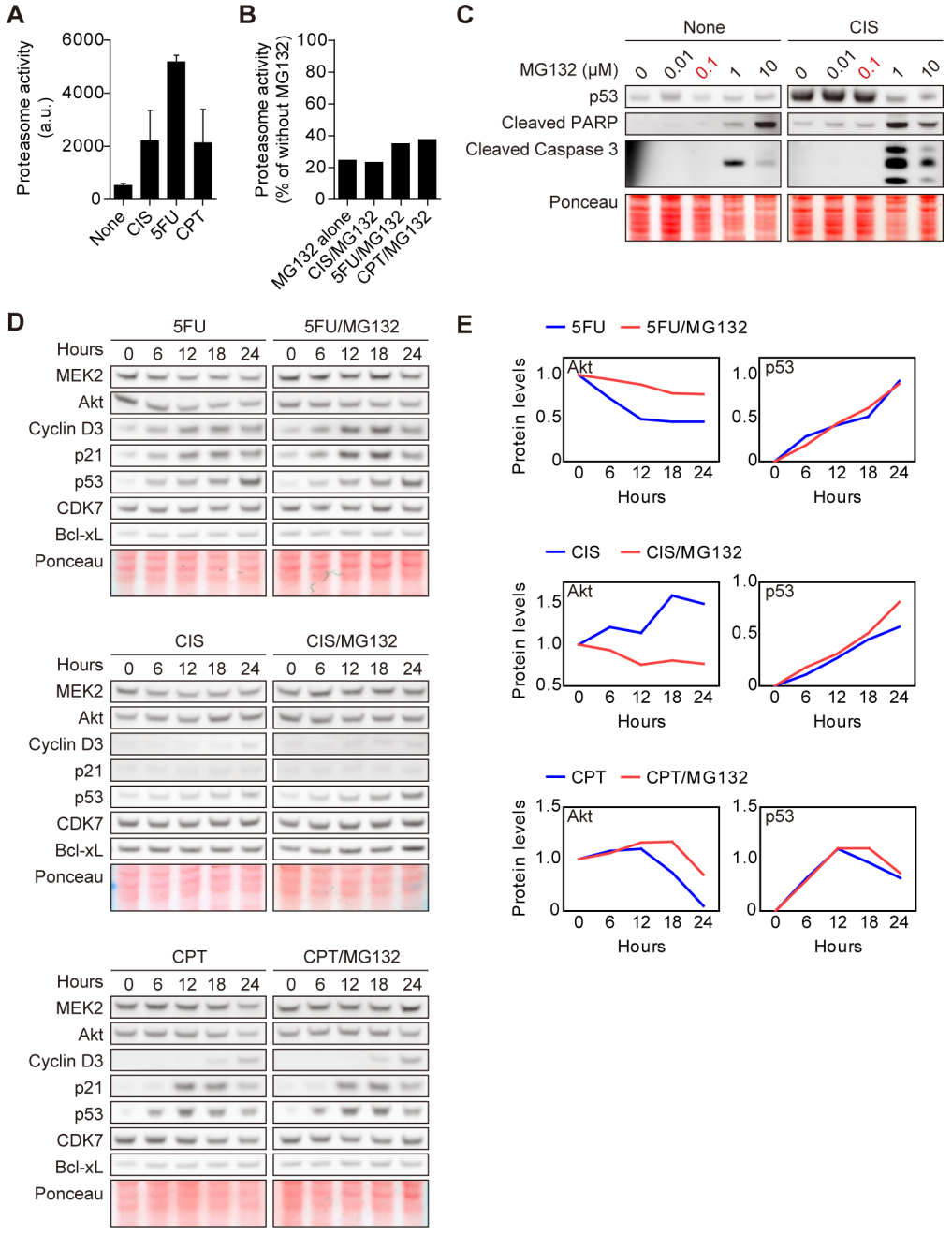

Figure 4. Altered protein dynamics by proteasome inhibitor. (A) Chymotripsin-like proteasome activity after genotoxic drug administration on HCT116 cells by a luciferase assay. Error bars indicate standard error of each set of triplicates. None, without drugs; A.U., arbitrary unit. (B) Effects of MG132 (0.1 μM) for proteasome activity in response to genotoxic drug administration represented the fraction of remaining activity. No error bars presented because the bars are the fraction calculated based on triplicated data of each set (with MG132/without MG132). (C) Proteasome inhibitor MG132 showed a minimum effect of p53 accumulation and apoptosis induction at the concentration of 0.1 μM in the presence of CIS (17 μM). Cells were treated with the indicated conditions for 24 h. Antibodies for protein detection are indicated at the left of each gel image. None, without drugs; Ponceau, Ponceau S staining. (D) Altered protein dynamics in response to CIS (17 μM), 5FU (40 μM), or CPT (300 μM) in the presence of 0.1 μM of MG132. Numbers indicated on the top of gel images are hours after drug administration. Antibodies for protein detection are indicated at the left of each gel image. Ponceau, Ponceau S staining. (E) Densitometric analysis of Western blots in Figure 4C. Protein levels of MEK2, Akt, Cyclin D3, and p53 were quantified relative to the highest signals of each treatment.

thereafter regardless of concentration or administration modes. However, sustained administration of CPT did not cause clear p53 stabilization, unlike 5FU and CIS, and instead induced oscillation of p53 levels. These results confirmed that the lysates used in the system were suitable for evaluating the protein dynamics of drug response.

Protein Dynamics Profile Reveals Distinct Patterns of Functionally Diverse Proteins

Once the system was validated by p53 dynamics, we classified all 666 protein dynamics (i.e., the average dynamics from 666 × 3 triplicate experiments) for 37 proteins over the course of 24 h. Thirty-eight percent of the protein profiles exhibited an increasing trend, whereas 32% exhibited a steady decrease over

DOI: 10.1021/acs.jproteome.5b00759
J. Proteome Res. 2016, 15, 205−215

time. The remainder of the protein profiles showed fluctuations (more than two peaks) within 24 h of the experiment. The classification of protein dynamics also revealed that peaks of protein levels shifted over time in response to each drug (Figure 2B).

Early peaks tended to be induced by low and medium concentrations of all drugs, which was consistent with the observation that these conditions did not induce marked cell death (Figure S4, Supporting Information). Rapid protein induction can be induced by drug concentrations that are sufficient to induce transcriptional activation, but still within the capacity for cells to detoxify the drug as well as continue to divide, which results in diluted concentrations of proteins.[27] High concentration of CIS and CPT induced a continuous increase in the numbers of protein levels, particularly those up to 24 h (i.e., protein dynamics peaked by 24 h) (Figure 2C, cluster *c* and *g* for CIS, cluster *e* for CPT). On the other hand, the administration mode used did not seem to affect the response peak (Figure 2D). This finding suggests that temporal drug administration is still effective for eliciting a protein response, including some proteins that peaked as late as 24 h.

Similarity Measurement of Protein Dynamics Implies the Involvement of Degradation Machinery for a Different Functional Range of Proteins

Disruption of the protein levels of components of the cell regulatory machinery can cause a global imbalance at the proteome level, which consequently induces apoptosis.[27] It has been hypothesized that a set of interacting proteins that are highly coexpressed (protein dynamics with a similar pattern over time) is likely to be a part of a functional module that performs a specific task.[13,15] Fluctuations of a regulatory protein level cause corresponding fluctuations of the partner protein levels when their interaction is active.[12,14] Alternatively, proteins that are regulated by the same molecule or molecules would also demonstrate high concordance. Furthermore, protein with similar degradation modes may also fluctuate with similar dynamics. Hence, correlations between changes in protein levels may provide information for potential regulatory connections without explicit perturbations of other cellular components.[12]

To evaluate the geometrical similarities of protein dynamics between two proteins, we applied the distance correlation (*dCor*).[10] Although the range of *dCor* ($0 \leq dCor \leq 1$) is similar to Pearson's correlation coefficient, *dCor* measures the dependence and tests the joint independence of two random vectors in an arbitrary dimension, even if they have a nonlinear relationship.[9] In the present data, *dCor* is one of the parameters that indicates a given pair of proteins "co-expressed" over a time axis in response to a particular drug administration condition. It can be a unique measurement of protein dynamics, as their level is also coregulated by the sum of protein synthesis, degradation, and dilution machinery from time to time.[27] Representative pairs of protein dynamics with *dCor* are shown in Figure 3A. In general, $dCor > 0.8$ indicates a reasonably similar geometry for a given pair of proteins.

An evaluation of *dCor* values for all possible 11,988 protein pairs within each drug administration combination (i.e., 666 protein dynamics × 18 conditions) revealed that the median *dCor* was 0.62 (range 0.21−0.99, Figure 3B). To confirm that the *dCor* is the product of a functional protein-dependent effect, the *dCor* between a protein detected by specific primary antibody and the corresponding total protein detected by colloidal gold was calculated. As expected, the *dCor* values for total protein were significantly lower than those represented by specific primary antibody pairs (Student *t*-test, $p < 0.0001$; Wolcoxon test, $p < 0.0001$, Figure 3C), suggesting that the protein level in response to anticancer drugs is regulated in a nonrandom manner. Among those detected by the specific primary antibody pairs, we also assessed *dCor* values based on whether the protein pair is known to interact based on information from the literature (i.e., "known interaction", Figure S5, Supporting Information). Interestingly, the average *dCor* did not significantly differ between known and unknown pairs (Student *t*-test, $p = 0.82$; Wilcoxon test, $p = 0.86$; Figure 3D and 3E). In fact, pairs showing >0.8 *dCor* also had 21.5% and 22.0% known and unknown pairs, respectively. These data suggest that the amount of known and unknown pairs of proteins may be regulated by degradation machinery that targets a wide functional range of proteins.

Alteration of Protein Dynamics by MG132

The continuous increase of a wide functional range of protein species has been reported to result from the down-regulation of degradation machinery.[27−30] Therefore, we hypothesized that the degradation system that targets a number of functionally different proteins plays a role in the response to drug-induced stress, instead of protein-specific degradation machinery.[31,32] Proteasome activity was increased by 4.0- to 9.9-fold after treatment with genotoxic drugs relative to no drug treatment (Figure 4A). A proteasome inhibitor, MG132, effectively reduced the proteasome activity by 20−40% relative to activity without 0.1 μM MG132 treatment (Figure 4B). Before initiating the proteasome inhibitory experiment, the antitumor effect of MG132 administered with CIS in terms of genotoxicity and apoptosis induction was assessed by measuring p53, cleaved PARP and cleaved caspase-3 levels. There was no visible genotoxic or apoptotic effects up to a concentration of 0.1 μM MG132 (Figure 4C). In addition, no remarkable morphological changes were observed after treatment with 0.1 μM MG132 and CIS (Figure S6, Supporting Information). These observations confirmed that 0.1 μM MG132 is appropriate for investigating the proteasome inhibitory effect in the presence of CIS at concentrations showing antitumor activity.

A subset of proteins (e.g., MEK2, Akt, Cyclin D3, p53, and p21) was chosen to monitor protein dynamics in the presence of MG132 by Western blot, in which the baseline dynamics to each drug were drug-unique. For example, CPT did not cause clear p53 stabilization, unlike 5FU and CIS. Both 5FU and CPT caused Akt degradation at different time points, whereas CIS induced Akt accumulation.

Inhibition of a proteasome system by MG132 increased the protein levels of MEK2 and Akt under 5FU, CIS, and CPT; however, MG132 did not affect the protein dynamics of Cyclin D3, p53, and p21 in the drug response (Figure 4D). Quantitative assessment of these dynamics confirmed the distinction of the effect of MG132 (Figure 4E). MG132 seemed to prevent or delay the protein degradation of Akt in cells treated with 5FU and CPT, whereas the Akt level after CIS treatment was suppressed by MG132. These results suggest that, at least in part, protein levels were regulated by a degradation system that targets a different functional range of proteins in the context of anticancer drug response.

Similarity in Protein Dynamics May Indicate Cellular Response and Progression of Apoptosis

We isolated 2,630 out of 11,988 protein pairs (22%) that exhibited *dCor* values above 0.80. The correlations were represented by a node-edge schematic,[23] in which proteins

DOI: 10.1021/acs.jproteome.5b00759
J. Proteome Res. 2016, 15, 205−215

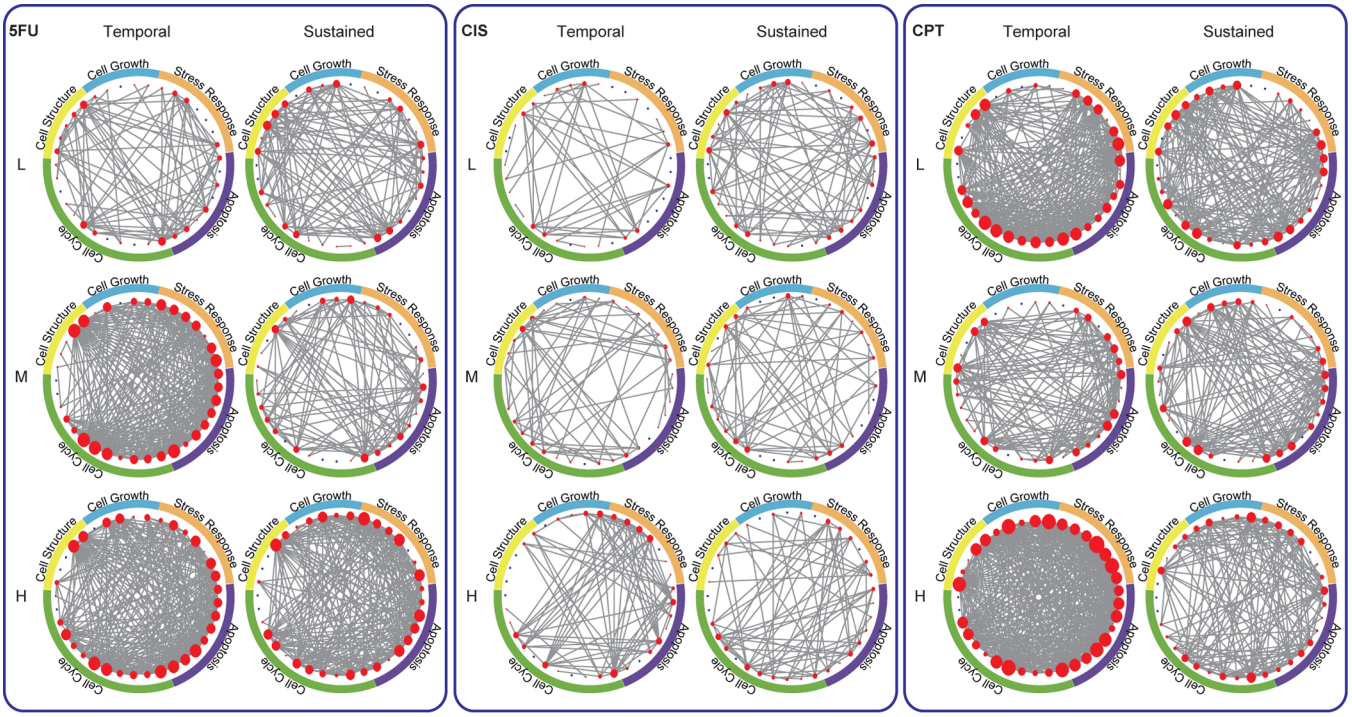

Figure 5. Representative node-edge illustrations of proteins showing similar dynamics defined by *dCor* > 0.80. Node-edge representation of functionally linked proteins under different conditions. Using protein level profile data obtained from the time-course experiments in response to 5FU, CIS, and CPT treatments at different concentrations and with different administration modes, distance correlation (*dCor*) was calculated for all possible protein pairs. Red circles (nodes) represent proteins, and lines (edges) represent connections between two proteins that have a *dCor* value >0.80. The size of the node indicates the number of edges connecting to that node, where larger nodes have more connections. The outer ring indicates the functional category designations for proteins, which are apoptosis, cell cycle, cell structure, cell growth, and stress response. L, M, and H indicate low, medium, and high drug concentrations, respectively. Each node represents a protein as follows (clockwise from Cell Structure proteins): TublinB, TublinA, MDR, CK7, CK19, MEK5, MEK2, GSK3β, ERK2, Akt, p90, p53, p53-Ser15, NF-κB, MKK7, MDM2, Chk2, TRADD, RIP, PARP, Caspase9, Caspase7, Caspase3, Caspase2, Bcl-xl, Rb, p21, p16, p15, CyclinE, CyclinD3, CyclinD1, CyclinB, CyclinA, CDK7, CDK4, and CDK2.

with similar dynamics (*dCor* > 0.80) were connected by an edge in the 15 functional category pairs across 18 conditions (Figure 5). Visual representations of connection nodes and edges showed an increasing trend in a concentration-depending manner for 5FU. Interestingly, CPT showed a greater number of connections at a low concentration compared to a moderate concentration. The low concentration of temporal drug administration was expected to induce minimum stress, but a large number of protein dynamics seemed to follow a stress response pattern. This finding suggests that low levels of genotoxic stress over a short period of time can still induce some systems that regulate protein levels. We also performed protein ontology enrichment analysis with respect to connection nodes. The number of connection nodes in the cell growth category was increased after the sustained administration mode for all drugs, while only CPT and 5FU exhibited a dose-dependent change in the number of connection nodes (Table S2, Supporting Information).

The connectivity of apoptosis and other functional protein pairs may indicate the progression of apoptosis, presumably by the cleavage of other proteins, such as structural proteins,[33] resulting in a decreased or fluctuated level of other proteins over time, possibly with a synchronized manner. In fact, the average *dCor* of pairs that had at least one apoptosis-related protein was significantly higher than those without the apoptosis-related proteins (Figure 6A). The average *dCor* increased in a dose-dependent manner (Figure 6B), and the temporal drug administration mode exhibited higher average *dCor* than the sustained administration mode (Figure 6C). These results suggest that apoptosis-related protease activity could also involve nonapoptosis-related protein degradation.[34] Further detailed observations of the *dCor* distribution by protein functional category pairs are illustrated in Figure S7, Supporting Information.

DISCUSSION

In the present study, we conducted a systems-level approach for understanding the drug response at the protein level to a variety of drug conditions over time. Among 12,000 time-course pairs, the similarity measurement of protein dynamics using *dCor* revealed that 22% of possible protein pairs were above 0.8, suggesting that the levels of multiple protein species were regulated in a synchronized fashion.[32,35] The mechanism appears to require a protein degradation system that targets multiple functionally unrelated proteins. We hypothesized that proteasome inhibitors should alter the protein dynamics in response to genotoxic drugs. As expected, the proteasome inhibitor, MG132, disrupted the expected protein dynamics in multiple protein species. From a protein function point-of-view, protein pairs possessing apoptosis-related proteins demonstrated significantly higher *dCor*, which confirmed that apoptosis-related cellular component deconstruction is associated with the proteasome.[36,37] Although these results obtained from HCT116 may be different in other cell lines, our present experimental and analytical pipelines demonstrated the utility of high-dimensional proteomic data in investigating the molecular response of cancer cells to genotoxic drugs.

DOI: 10.1021/acs.jproteome.5b00759
J. Proteome Res. 2016, 15, 205−215

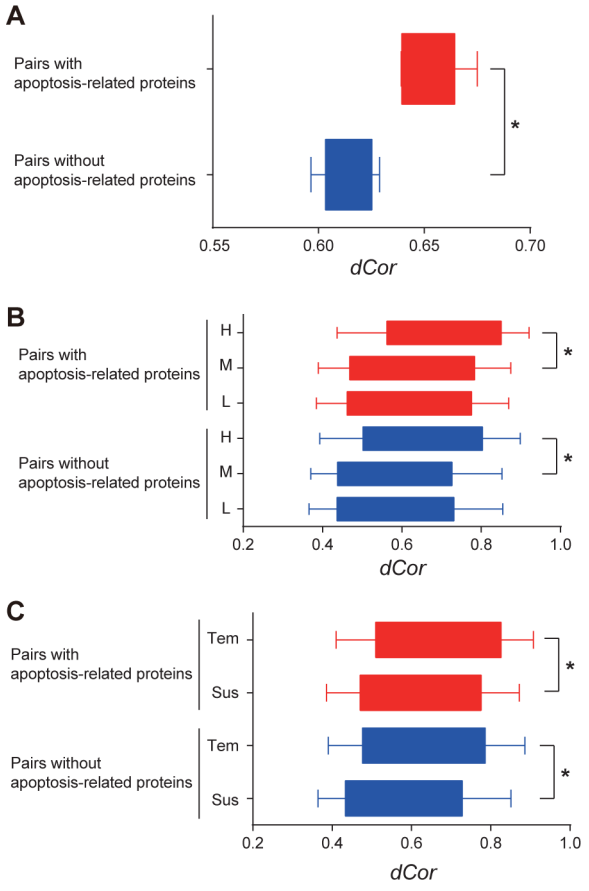

Figure 6. Distance correlations in protein pairs with or without apoptosis-related proteins. (A) Comparison of average *dCor* values. Asterisk indicates $p < 0.05$ from student *t*-test. (B) Comparison of average *dCor* values by drug concentrations. Asterisk indicates $p < 0.05$ from student *t*-test. (C) Comparison of average *dCor* values by drug administration modes. Asterisk indicates $p < 0.05$ from student *t*-test.

To date, several approaches have been introduced in the context of molecular response dynamics monitoring, such as Western blot,[38] cell-based kinase assays,[39] LC-MS/MS,[40] sandwich immunoassays,[41] and lysate arrays.[42] These techniques have mainly been used to measure cellular signaling with growth factors and hormones, and thus one is limited to focusing on a relatively small number of pathways involving numerous phosphorylated proteins for the use of molecular targeting agents, rather than complex networks triggered by cellular damage. Conventional anticancer drugs (e.g., 5FU, CIS, and CPT), which are still a mainstay for most cancer chemotherapies, impart genotoxic stress as their general mechanism of action.[43] Importantly, most of these agents have not been specifically designed to bind particular molecular targets.[44] The response to anticancer drugs appears to be a hyperdynamic state in which thousands of protein species alter their levels through increased and decreased degradation.[27] In general, *de novo* synthesized proteins are exposed to various intracellular conditions that lead to degradation in proteasome pathways, which is triggered by a variety of cellular events, including chemical damage.[45] Hence, the molecular effects of drugs would involve nonspecific or passive reactions resulting in a change of protein levels. Molecular events induced by anticancer agents should therefore consist of degradation machinery-regulated changes in protein levels, rather than changes in a few important pathways.[46]

It is crucial to monitor global protein dynamics in a comprehensive manner. With respect to monitoring protein dynamics comprehensively, RPPA may be comparable to the CD-tagging technique.[47,48] The CD-tagging technique tags proteins at their endogenous chromosomal locations, thus allowing researchers to trace proteins localized within the original subcellular fractions with fluorescent markers regulated by their native promoter.[49] The localization and degradation of a large set of proteins from over 1,200 CD-tagging clones in response to CPT over a time-course at the single cell level has already been investigated.[11,27] In contrast, RPPA is a lysate-based technique that sacrifices morphological and single cell information;[4,5] however, to print an array of RPPA, only 10–100 pL of the lysate is required per spot.[6] As a result, RPPA allows one to examine a number of different protein species by antibodies from a portion of the identical cell lysate of different conditions (e.g., time-course).[17,50−54] Another advantage of RPPA is that cells are not affected by exogenous processing. It does not require genetic engineering or a change in medium to the cells, and thus, the data are the product of endogenous effects on the cells from a variety of cellular stimuli. In addition, the specific advantage of antibody-based techniques is that the antigens are almost fully characterized, which makes function-based profiling feasible.

Based on the idea that a set of coexpressed pairs from a comprehensive protein list is likely to form a functional module that implements a specific cellular demand,[11,13,14,49] we employed the *dCor* parameter to measure the similarity of dynamics between a given pair of proteins. Our results partially support the hypothesis that functionally similar proteins show similar dynamics over time.[11] However, the proteasome inhibitor MG132 induced variation in protein dynamics among proteins with different functions. This finding suggests that proteins are regulated by the proteasome system regardless of protein functions. However, compared to the list of proteins presented in the CD-tagging protein library,[11] our antibody-based detection method may still possess a selection bias, which may result in a greater chance of detecting proteins expressed at low levels.

In summary, our results indicate that RPPA is an effective method for monitoring the overarching trends in protein dynamics during drug treatment. A substantial portion of proteins demonstrated similar dynamics, which has been hypothesized to be due to protein degradation machinery targeting multiple functionally diverse proteins. The mechanism that regulates protein levels through degradation may be a plausible counterpart of molecular targeting agents.[55−58] In the present study, the response to genotoxic drugs was demonstrated with only one cell line, HCT116. Accumulation of such multidimensional protein dynamics data on a broad range of cell lines will enable an understanding of detailed mechanisms of drug action, which will eventually contribute to in silico modeling for anticancer drugs. Accumulation of such multidimensional protein dynamics data on a broad range of cell lines will enable an understanding of the detailed mechanisms of drug action, which will eventually contribute to *in silico* modeling for anticancer drug therapy.

DOI: 10.1021/acs.jproteome.5b00759
J. Proteome Res. 2016, 15, 205−215

■ ASSOCIATED CONTENT

Supporting Information

The Supporting Information is available free of charge on the ACS Publications website at DOI: 10.1021/acs.jproteome.5b00759.

Antibody specificity screening by strip Western blot (Figure S1); Confirmation of drug response by conventional Western blot (Figure S2); Bias removal using principal component analysis (PCA) (Figure S3); Cell cycle arrest and apoptosis induced by 5FU, CIS, and CPT (Figure S4); Summary of protein−protein interactions based on the literature search (Figure S5); Morphology of HCT116 used in Figure 4B (Figure S6); Distribution of distance correlation depending on conditions based on protein function (Figure S7); Primary antibodies used for quantitative protein detection using RPPA (Table S1); Enrichment of functional nodes on drug administration modes (Table S2) (PDF). (PDF)

■ AUTHOR INFORMATION

Corresponding Author

*(S.S.N.) E-mail: snishizu@iwate-med.ac.jp; Phone: +81 (19) 651 5111.

Author Contributions

S.S.N. conceived and designed experiments. K.K., K.I., M.I., T.S., and S.S.N. performed biological experiments. K.K., K.T., L.Y., and S.S.N. analyzed data. K.K. and S.S.N. wrote the manuscript.

Notes

The authors declare no competing financial interest.

■ ACKNOWLEDGMENTS

This work was supported by a Keiryokai Research Foundation (101) grant to S.S.N.; a KAKENHI (21591676) Grant-in-Aid for Scientific Research (C) to S.S.N.; the MIAST (Medical Innovation by Advanced Science and Technology) project of the Ministry of Education, Culture, Sports, Science and Technology, Japan, to K.K. and S.S.N.; and a research fund from The Japan Prize Foundation to K.K. We thank Hirotoshi Nakajima of Iwate Prefectural University for artwork. We would like to thank Cindy Clark, NIH Library Editing Service, for reviewing the manuscript.

■ ABBREVIATIONS

CIS, cisplatin; 5FU, 5-fluorouracil; CPT, CPT-11 (irinotecan); RPPA, reverse-phase protein microarray; *dCor*, correlation distance; GI_{50}, 50% growth suppression; tem, temporal mode; sus, sustained mode; CV, coefficient of variation; PCA, principal component analysis; MC/MC, Morkov Chain Monte Carlo

■ REFERENCES

(1) Bouwman, P.; Jonkers, J. The effects of deregulated DNA damage signalling on cancer chemotherapy response and resistance. *Nat. Rev. Cancer* **2012**, *12*, 587−598.

(2) Polo, S. E.; Jackson, S. P. Dynamics of DNA damage response proteins at DNA breaks: a focus on protein modifications. *Genes Dev.* **2011**, *25*, 409−433.

(3) Clarke, R.; Ressom, H. W.; Wang, A.; Xuan, J.; Liu, M. C.; Gehan, E. A.; Wang, Y. The properties of high-dimensional data spaces: implications for exploring gene and protein expression data. *Nat. Rev. Cancer* **2008**, *8*, 37−49.

(4) Nishizuka, S.; Charboneau, L.; Young, L.; Major, S.; Reinhold, W. C.; Waltham, M.; Kouros-Mehr, H.; Bussey, K. J.; Lee, J. K.; Espina, V.; Munson, P. J.; Petricoin, E., 3rd; Liotta, L. A.; Weinstein, J. N. Proteomic profiling of the NCI-60 cancer cell lines using new high-density reverse-phase lysate microarrays. *Proc. Natl. Acad. Sci. U. S. A.* **2003**, *100*, 14229−14234.

(5) Paweletz, C. P.; Charboneau, L.; Bichsel, V. E.; Simone, N. L.; Chen, T.; Gillespie, J. W.; Emmert-Buck, M. R.; Roth, M. J.; Petricoin, I. E.; Liotta, L. A. Reverse phase protein microarrays which capture disease progression show activation of pro-survival pathways at the cancer invasion front. *Oncogene* **2001**, *20*, 1981−1989.

(6) Spurrier, B.; Ramalingam, S.; Nishizuka, S. Reverse-phase protein lysate microarrays for cell signaling analysis. *Nat. Protoc.* **2008**, *3*, 1796−1808.

(7) Spurrier, B.; Washburn, F. L.; Asin, S.; Ramalingam, S.; Nishizuka, S. Antibody screening database for protein kinetic modeling. *Proteomics* **2007**, *7*, 3259−3263.

(8) Major, S. M.; Nishizuka, S.; Morita, D.; Rowland, R.; Sunshine, M.; Shankavaram, U.; Washburn, F.; Asin, D.; Kouros-Mehr, H.; Kane, D.; Weinstein, J. N. AbMiner: a bioinformatic resource on available monoclonal antibodies and corresponding gene identifiers for genomic, proteomic, and immunologic studies. *BMC Bioinf.* **2006**, *7*, 192.

(9) Székely, G. J.; Rizzo, M. L. Brownian distance covariance. *Ann. Appl. Stat* **2009**, *3*, 1236−1265.

(10) Székely, G. J.; Rizzo, M. L.; Bakirov, N. K. Measuring and testing dependence by correlation of distances. *Ann. Stat* **2007**, *35*, 2769−2794.

(11) Cohen, A. A.; Geva-Zatorsky, N.; Eden, E.; Frenkel-Morgenstern, M.; Issaeva, I.; Sigal, A.; Milo, R.; Cohen-Saidon, C.; Liron, Y.; Kam, Z.; Cohen, L.; Danon, T.; Perzov, N.; Alon, U. Dynamic proteomics of individual cancer cells in response to a drug. *Science* **2008**, *322*, 1511−1516.

(12) Dunlop, M. J.; Cox, R. S., 3rd; Levine, J. H.; Murray, R. M.; Elowitz, M. B. Regulatory activity revealed by dynamic correlations in gene expression noise. *Nat. Genet.* **2008**, *40*, 1493−1498.

(13) Goel, A.; Li, S. S.; Wilkins, M. R. Four-dimensional visualisation and analysis of protein-protein interaction networks. *Proteomics* **2011**, *11*, 2672−2682.

(14) Komurov, K.; White, M. Revealing static and dynamic modular architecture of the eukaryotic protein interaction network. *Mol. Syst. Biol.* **2007**, *3*, 110.

(15) Segal, E.; Wang, H.; Koller, D. Discovering molecular pathways from protein interaction and gene expression data. *Bioinformatics* **2003**, *19* (Suppl 1), i264−271.

(16) Nishizuka, S. Profiling cancer stem cells using protein array technology. *Eur. J. Cancer* **2006**, *42*, 1273−1282.

(17) Nishizuka, S.; Ramalingam, S.; Spurrier, B.; Washburn, F. L.; Krishna, R.; Honkanen, P.; Young, L.; Tsutomu, S.; Steeg, P. S.; Austin, J. Quantitative protein network monitoring in response to DNA damage. *J. Proteome Res.* **2008**, *7*, 803−808.

(18) Benito, M.; Parker, J.; Du, Q.; Wu, J.; Xiang, D.; Perou, C. M.; Marron, J. S. Adjustment of systematic microarray data biases. *Bioinformatics* **2004**, *20*, 105−114.

(19) Lombardi, M. Bayesian inference for α-stable distributions: A randomwalkMCMC approach. *Comput. Stat Data Anal* **2007**, *51*, 2688−2700.

(20) Sturn, A.; Mlecnik, B.; Pieler, R.; Rainer, J.; Truskaller, T.; Trajanoski, Z. Client-server environment for high-performance gene expression data analysis. *Bioinformatics* **2003**, *19*, 772−773.

(21) Scherf, U.; Ross, D. T.; Waltham, M.; Smith, L. H.; Lee, J. K.; Tanabe, L.; Kohn, K. W.; Reinhold, W. C.; Myers, T. G.; Andrews, D. T.; Scudiero, D. A.; Eisen, M. B.; Sausville, E. A.; Pommier, Y.; Botstein, D.; Brown, P. O.; Weinstein, J. N. A gene expression database for the molecular pharmacology of cancer. *Nat. Genet.* **2000**, *24*, 236−244.

(22) Weinstein, J. N.; Myers, T. G.; O'Connor, P. M.; Friend, S. H.; Fornace, A. J., Jr.; Kohn, K. W.; Fojo, T.; Bates, S. E.; Rubinstein, L. V.; Anderson, N. L.; Buolamwini, J. K.; van Osdol, W. W.; Monks, A. P.; Scudiero, D. A.; Sausville, E. A.; Zaharevitz, D. W.; Bunow, B.; Viswanadhan, V. N.; Johnson, G. S.; Wittes, R. E.; Paull, K. D. An

DOI: 10.1021/acs.jproteome.5b00759
J. Proteome Res. 2016, 15, 205−215

information-intensive approach to the molecular pharmacology of cancer. *Science* **1997**, *275*, 343−349.
(23) Gehlenborg, N.; Wong, B. Points of view: networks. *Nat. Methods* **2012**, *9*, 115.
(24) Shimura, T.; Toyoshima, M.; Adiga, S. K.; Kunoh, T.; Nagai, H.; Shimizu, N.; Inoue, M.; Niwa, O. Suppression of replication fork progression in low-dose-specific p53-dependent S-phase DNA damage checkpoint. *Oncogene* **2006**, *25*, 5921−5932.
(25) Halazonetis, T. D.; Gorgoulis, V. G.; Bartek, J. An oncogene-induced DNA damage model for cancer development. *Science* **2008**, *319*, 1352−1355.
(26) Reinhardt, H. C.; Schumacher, B. The p53 network: cellular and systemic DNA damage responses in aging and cancer. *Trends Genet.* **2012**, *28*, 128−136.
(27) Eden, E.; Geva-Zatorsky, N.; Issaeva, I.; Cohen, A.; Dekel, E.; Danon, T.; Cohen, L.; Mayo, A.; Alon, U. Proteome half-life dynamics in living human cells. *Science* **2011**, *331*, 764−768.
(28) Yang, Y.; Kitagaki, J.; Wang, H.; Hou, D. X.; Perantoni, A. O. Targeting the ubiquitin-proteasome system for cancer therapy. *Cancer Sci.* **2009**, *100*, 24−28.
(29) Pagano, M.; Benmaamar, R. When protein destruction runs amok, malignancy is on the loose. *Cancer Cell* **2003**, *4*, 251−256.
(30) Hernandez, A. R.; Klein, A. M.; Kirschner, M. W. Kinetic responses of beta-catenin specify the sites of Wnt control. *Science* **2012**, *338*, 1337−1340.
(31) DeMartino, G. N.; Slaughter, C. A. The proteasome, a novel protease regulated by multiple mechanisms. *J. Biol. Chem.* **1999**, *274*, 22123−22126.
(32) Ablain, J.; Nasr, R.; Bazarbachi, A.; de The, H. The drug-induced degradation of oncoproteins: an unexpected Achilles' heel of cancer cells? *Cancer Discovery* **2011**, *1*, 117−127.
(33) Tao, G. Z.; Li, D. H.; Zhou, Q.; Toivola, D. M.; Strnad, P.; Sandesara, N.; Cheung, R. C.; Hong, A.; Omary, M. B. Monitoring of epithelial cell caspase activation via detection of durable keratin fragment formation. *J. Pathol.* **2008**, *215*, 164−174.
(34) Lamkanfi, M.; Festjens, N.; Declercq, W.; Vanden Berghe, T.; Vandenabeele, P. Caspases in cell survival, proliferation and differentiation. *Cell Death Differ.* **2007**, *14*, 44−55.
(35) Stathopoulou, A.; Roukos, V.; Petropoulou, C.; Kotsantis, P.; Karantzelis, N.; Nishitani, H.; Lygerou, Z.; Taraviras, S. Cdt1 is differentially targeted for degradation by anticancer chemotherapeutic drugs. *PLoS One* **2012**, *7*, e34621.
(36) Orlowski, R. Z.; Kuhn, D. J. Proteasome inhibitors in cancer therapy: Lessons from the first decade. *Clin. Cancer Res.* **2008**, *14*, 1649−1657.
(37) Sherman, M. Y.; Goldberg, A. L. Cellular defenses against unfolded proteins: a cell biologist thinks about neurodegenerative diseases. *Neuron* **2001**, *29*, 15−32.
(38) Kubota, H.; Noguchi, R.; Toyoshima, Y.; Ozaki, Y.; Uda, S.; Watanabe, K.; Ogawa, W.; Kuroda, S. Temporal coding of insulin action through multiplexing of the AKT pathway. *Mol. Cell* **2012**, *46*, 820−832.
(39) Miller-Jensen, K.; Janes, K. A.; Brugge, J. S.; Lauffenburger, D. A. Common effector processing mediates cell-specific responses to stimuli. *Nature* **2007**, *448*, 604−608.
(40) Isabelle, M.; Gagne, J. P.; Gallouzi, I. E.; Poirier, G. G. Quantitative proteomics and dynamic imaging reveal that G3BP-mediated stress granule assembly is poly(ADP-ribose)-dependent following exposure to MNNG-induced DNA alkylation. *J. Cell Sci.* **2012**, *125*, 4555−4566.
(41) Korf, U.; Derdak, S.; Tresch, A.; Henjes, F.; Schumacher, S.; Schmidt, C.; Hahn, B.; Lehmann, W. D.; Poustka, A.; Beissbarth, T.; Klingmuller, U. Quantitative protein microarrays for time-resolved measurements of protein phosphorylation. *Proteomics* **2008**, *8*, 4603−4612.
(42) Sevecka, M.; Wolf-Yadlin, A.; MacBeath, G. Lysate microarrays enable high-throughput, quantitative investigations of cellular signaling. *Mol. Cell. Proteomics* **2011**, *10*, M110.005363.
(43) Curtin, N. J. DNA repair dysregulation from cancer driver to therapeutic target. *Nat. Rev. Cancer* **2012**, *12*, 801−817.
(44) Schneider, G.; Fechner, U. Computer-based de novo design of drug-like molecules. *Nat. Rev. Drug Discovery* **2005**, *4*, 649−663.
(45) Goldberg, A. L. Protein degradation and protection against misfolded or damaged proteins. *Nature* **2003**, *426*, 895−899.
(46) Glickman, M. H.; Ciechanover, A. The ubiquitin-proteasome proteolytic pathway: destruction for the sake of construction. *Physiol. Rev.* **2002**, *82*, 373−428.
(47) Cohen, A. A.; Kalisky, T.; Mayo, A.; Geva-Zatorsky, N.; Danon, T.; Issaeva, I.; Kopito, R. B.; Perzov, N.; Milo, R.; Sigal, A.; Alon, U. Protein dynamics in individual human cells: experiment and theory. *PLoS One* **2009**, *4*, e4901.
(48) Jarvik, J. W.; Adler, S. A.; Telmer, C. A.; Subramaniam, V.; Lopez, A. J. CD-tagging: a new approach to gene and protein discovery and analysis. *Biotechniques* **1996**, *20*, 896−904.
(49) Sigal, A.; Milo, R.; Cohen, A.; Geva-Zatorsky, N.; Klein, Y.; Liron, Y.; Rosenfeld, N.; Danon, T.; Perzov, N.; Alon, U. Variability and memory of protein levels in human cells. *Nature* **2006**, *444*, 643−646.
(50) Albeck, J. G.; MacBeath, G.; White, F. M.; Sorger, P. K.; Lauffenburger, D. A.; Gaudet, S. Collecting and organizing systematic sets of protein data. *Nat. Rev. Mol. Cell Biol.* **2006**, *7*, 803−812.
(51) Nieto-Barajas, L. E.; Muller, P.; Ji, Y.; Lu, Y.; Mills, G. B. A time-series DDP for functional proteomics profiles. *Biometrics* **2012**, *68*, 859−868.
(52) Ramalingam, S.; Honkanen, P.; Young, L.; Shimura, T.; Austin, J.; Steeg, P. S.; Nishizuka, S. Quantitative assessment of the p53-Mdm2 feedback loop using protein lysate microarrays. *Cancer Res.* **2007**, *67*, 6247−6252.
(53) Winters, M. E.; Mehta, A. I.; Petricoin, E. F., 3rd; Kohn, E. C.; Liotta, L. A. Supra-additive growth inhibition by a celecoxib analogue and carboxyamido-triazole is primarily mediated through apoptosis. *Cancer Res.* **2005**, *65*, 3853−3860.
(54) Lee, M. J.; Ye, A. S.; Gardino, A. K.; Heijink, A. M.; Sorger, P. K.; MacBeath, G.; Yaffe, M. B. Sequential application of anticancer drugs enhances cell death by rewiring apoptotic signaling networks. *Cell* **2012**, *149*, 780−794.
(55) Emanuele, M. J.; Elia, A. E.; Xu, Q.; Thoma, C. R.; Izhar, L.; Leng, Y.; Guo, A.; Chen, Y. N.; Rush, J.; Hsu, P. W.; Yen, H. C.; Elledge, S. J. Global identification of modular cullin-RING ligase substrates. *Cell* **2011**, *147*, 459−474.
(56) Adams, J. The development of proteasome inhibitors as anticancer drugs. *Cancer Cell* **2004**, *5*, 417−421.
(57) Du, W.; Mei, Q. B. Ubiquitin-proteasome system, a new anti-tumor target. *Acta Pharmacol. Sin.* **2013**, *34*, 187−188.
(58) Cho-Park, P. F.; Steller, H. Proteasome regulation by ADP-ribosylation. *Cell* **2013**, *153*, 614−627.

DOI: 10.1021/acs.jproteome.5b00759
J. Proteome Res. 2016, 15, 205−215